NAVAL POSTGRADUATE SCHOOL

MONTEREY, CALIFORNIA

THESIS

WIRELESS IR IMAGE TRANSFER SYSTEM FOR AUTONOMOUS VEHICLE

by

Ali Ata

December 2003

Thesis Advisor:	Gamani Karunasiri
Co Advisor :	Richard M. Harkins

Approved for public release; distribution is unlimited

THIS PAGE INTENTIONALLY LEFT BLANK

REPORT DOCUMENTATION PAGE			*Form Approved OMB No. 0704-0188*
Public reporting burden for this collection of information is estimated to average 1 hour per response, including the time for reviewing instruction, searching existing data sources, gathering and maintaining the data needed, and completing and reviewing the collection of information. Send comments regarding this burden estimate or any other aspect of this collection of information, including suggestions for reducing this burden, to Washington headquarters Services, Directorate for Information Operations and Reports, 1215 Jefferson Davis Highway, Suite 1204, Arlington, VA 22202-4302, and to the Office of Management and Budget, Paperwork Reduction Project (0704-0188) Washington DC 20503.			
1. AGENCY USE ONLY *(Leave blank)*	**2. REPORT DATE** December 2003	**3. REPORT TYPE AND DATES COVERED** Master's Thesis	
4. TITLE AND SUBTITLE: Wireless IR Image Transfer System for Autonomous Vehicles			**5. FUNDING NUMBERS**
6. AUTHOR(S) Ali ATA			
7. PERFORMING ORGANIZATION NAME(S) AND ADDRESS(ES) Naval Postgraduate School Monterey, CA 93943-5000			**8. PERFORMING ORGANIZATION REPORT NUMBER**
9. SPONSORING /MONITORING AGENCY NAME(S) AND ADDRESS(ES) N/A			**10. SPONSORING/MONITORING AGENCY REPORT NUMBER**
11. SUPPLEMENTARY NOTES The views expressed in this thesis are those of the author and do not reflect the official policy or position of the Department of Defense or the U.S. Government.			
12a. DISTRIBUTION / AVAILABILITY STATEMENT Approved for public release; distribution is unlimited			**12b. DISTRIBUTION CODE**

13. ABSTRACT (maximum 200 words)

A wireless IR image transfer mechanism was developed and tested for eventual employment on the NPS autonomous ground vehicle. Tests were conducted inside a building as a rough simulation of an urban environment. Two common ISM frequency bands were explored. Experiments results proved that the 915 MHz band was best suited for this effort. Data revealed that minimal signal loss occurs at Line of Site out to several hundred meters. Signal loss through obstructions: Cement, wood, and metal proved significant, on the order of 10 –15 dB per obstruction. But the image transfer was successful through multiple obstructions at range of 400 meters. Further work includes integration into the autonomous vehicle and testing of the performance.

14. SUBJECT TERMS Infrared Imaging, Serial Communication, Antenna Polarization			**15. NUMBER OF PAGES** 49
			16. PRICE CODE
17. SECURITY CLASSIFICATION OF REPORT Unclassified	**18. SECURITY CLASSIFICATION OF THIS PAGE** Unclassified	**19. SECURITY CLASSIFICATION OF ABSTRACT** Unclassified	**20. LIMITATION OF ABSTRACT** UL

NSN 7540-01-280-5500

Standard Form 298 (Rev. 2-89)
Prescribed by ANSI Std. 239-18

THIS PAGE INTENTIONALLY LEFT BLANK

Approved for public release; distribution is unlimited

WIRELESS IR THERMAL IMAGE TRANSFER SYSTEM FOR AUTONOMOUS VEHICLES

Ali ATA
Lieutenant Junior Grade Turkish Navy
B.S., Turkish Naval Academy, 1997

Submitted in partial fulfillment of the
requirements for the degree of

MASTER OF SCIENCE IN APPLIED PHYSICS

from the

NAVAL POSTGRADUATE SCHOOL
December2003

Author: Ali ATA

Approved by: Gamani Karunasiri
Thesis Advisor

Richard Harkins
Co-Advisor

James Luscombe
Chairman, Department of Physics

THIS PAGE INTENTIONALLY LEFT BLANK

ABSTRACT

A wireless IR image transfer mechanism was developed and tested for eventual employment on the NPS autonomous ground vehicle. Tests were conducted inside a building as a rough simulation of an urban environment. Two common ISM frequency bands were explored. Experiments results proved that the 915 MHz band was best suited for this effort. Data revealed that minimal signal loss occurs at Line of Site out to several hundred meters. Signal loss through obstructions: Cement, wood, and metal proved significant, on the order of 10 –15 dB per obstruction. But the image transfer was successful through multiple obstructions at range of 400 meters. Further work includes integration into the autonomous vehicle and testing of the performance.

THIS PAGE INTENTIONALLY LEFT BLANK

TABLE OF CONTENTS

THIS PAGE INTENTIONALLY LEFT BLANK

LIST OF FIGURES

THIS PAGE INTENTIONALLY LEFT BLANK

LIST OF TABLES

THIS PAGE INTENTIONALLY LEFT BLANK

ACKNOWLEDGMENTS

I would like to thank Prof. Gamani Karunasiri and Richard Harkins for their valuable support and their continuous help to make everything clearer during my thesis work. Professor Gamani’s experiences about IR theory and Richard Harkin’s background about wireless systems have led me successfully finish my thesis. I also need to thank my two budies Fatih Pala and Kurtulus Bektas for their friendship and help.I want to express my special appreciations to the TURKISH Nation and Turkish Naval Forces for providing this opportunity of education here.

In my last sentences I would like to thank my parents and my wife Arzu for their support and help. Arzu, my wife has been always up when I was down, with her courage and her love during these two years; be with me to the end of my life.

THIS PAGE INTENTIONALLY LEFT BLANK

I. BACKGROUND

A. INTRODUCTION

This thesis describes a wireless IR image transfer mechanism that was developed and tested for autonomous ground vehicles. This mechanism allows the autonomous vehicle operate under complete darkness for example inside caves.

A wireless IR image transfer mechanism as illustrated schematically in Figure 1 was developed and tested for eventual employment on an autonomous ground vehicle.

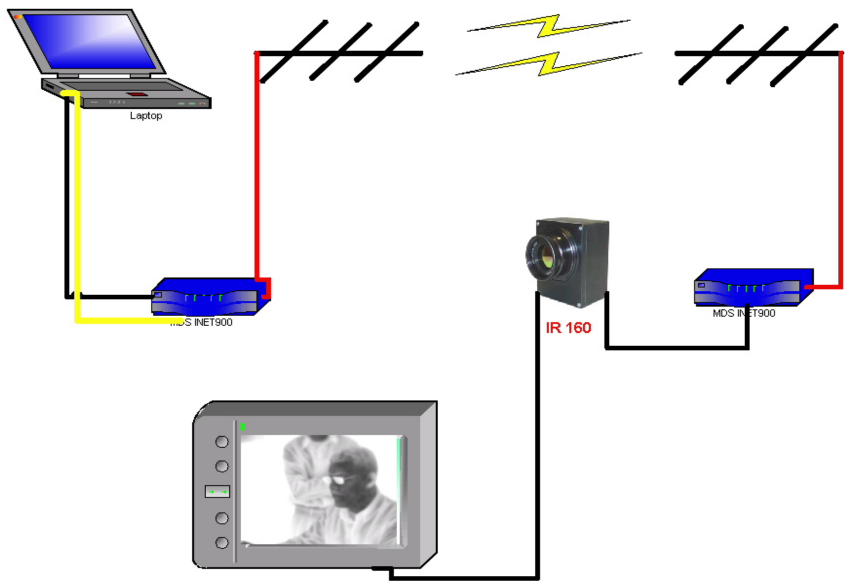

Figure 1. Block diagram of the system.

Two common Industrial, Scientific and Medical (ISM) frequency bands, 2.4 GHz and 915 MHz, were explored for performance testing. The main goal of the project was to successfully demonstrate long-range IR image transfer under different operating environments. The system consists of an uncooled infrared camera, two antennas and two transceivers.

B. SYSTEM COMPONENTS

1. Un-cooled IR Camera

The heart of the imaging system is the IR–160 Thermal Camera, manufactured by Infrared Solutions Inc., Figure 2.

Figure 2. IR – 160 Infrared camera.

The IR–160 imager provides a 160 x 120 pixel NTCS or PAL video output signal. The camera is sensitive to the long wave infrared band and has a temperature resolution under 0.08 ^{0} C with its f / 0.8 lens. The imager can automatically adjust the brightness and contrast of the video output signal, or may be remotely commanded, via its RS-232serial communication link, to select preprogrammed and custom palettes, to optimize the image for application. The performance characteristics of the camera are listed in Table 1.

PARTS	PROPERTIES
Detector	160(H) x 120(V) microbolometer focal plane array with CMOS ROIC
Pixel Size	50 micrometer square pixel
A/D Conversion	14 bit Digitizing resolution
Cryogenic Cooling	None required
FOV	22.9 0 (H) x 17.2 0 (V) with 20 mm focal length lens
IFOV	4.0 mrad with 20 mm focal length lens
Lens	Germanium 20 mm,F/0.8,focus 12" to infinity
Spectral Band	8 - 14 micrometer, anti reflection coated Germanium optics
NETD	<60 mk @ 300 C
Radiometric	Future capability
Moving Parts	Intermittent shutter
Operating Temperature	0 to 50 0 C
Power Input	9.0 24.0 VDC,< 5 Watts with shutter open
Frame R ate	30 Hz.
Communication	RS – 232
Video Output	NTCS or PAL composite video outputs
Functions	Contrast, Brightness, Freeze Frame, Palette Selection
Engine Size	3.0 x 3.0 x1.5 in.
Engine Weight	< 5.0 oz.
Housing Size	4.3 x 3.9 x 4.2 in.(W xH x D)
Complete Imager Weight	24.0 oz without lens
Mounting Orientation	Any orientation

Table 1. The Specs of the camera [from Ref. 4].

Since uncooled microbolometer technology does not need external cooling, the camera can operate between 0 and 50^0 C; this uniquely suites it for employment on autonomous vehicles in rugged environments.

The camera is based on a microbolometer sensor array that does not require a mechanical radiation chopper as commonly used in pyroelectric based sensors. This is advantage for robotic application where the power consumption should be minimized.

The main idea of the microbolometer is to convert a temperature difference to voltage difference. The structure of the microbolometer consists of a thermally isolated resistor made of a material, which has a high temperature coefficient of resistance.

A typical microbolometer pixel is illustrated in Figure 3. [11]

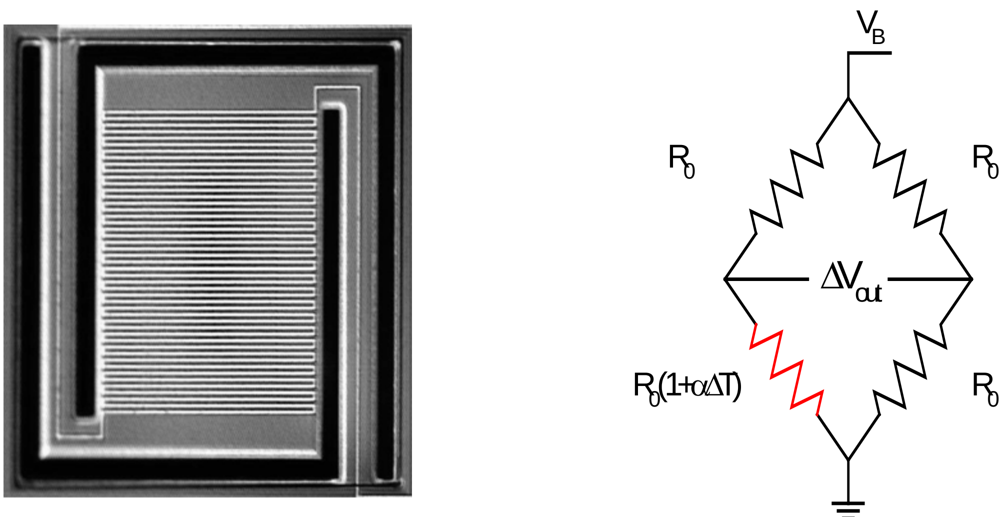

Figure 3. Microbolometer pixel and its readout circuit.

The amount of resistance change due to incident infrared is usually probed using a Wheatstone bridge and the output voltage of the bridge can be obtained as; [11]

$$\triangle V_{out} \approx \alpha * (V_B / 4) * \triangle T \qquad (1.1)$$

Where;

α = Coefficient of the temperature resistance.

V_B = Amplitude of the bias voltage

R_0 = Resistance of the microbolometer at room temperature

$\triangle T$ = Time difference of the microbolometer

$R_0\ (1+\alpha\triangle T)$ =Thermally isolated resistor of the microbolometer

The circuit shown in Figure 3 is a Wheatstone bridge including one microbolometer and three reference resistors.

At room temperature, the four arms of the bridge have identical resistance values so that the output voltage, $\triangle V_{out}$ is equal to zero. When a square voltage pulse is applied to the bridge, the resistance of the bolometer changes as a result of self-heating due to high thermal isolation while the resistance of the three reference resistors practically remains the same. Under infrared illumination, the resistance of the microbolometer changes and the amount of change can be sensed applying a voltage pulse V_B across the bridge. [11].

2. YAGI Antenna

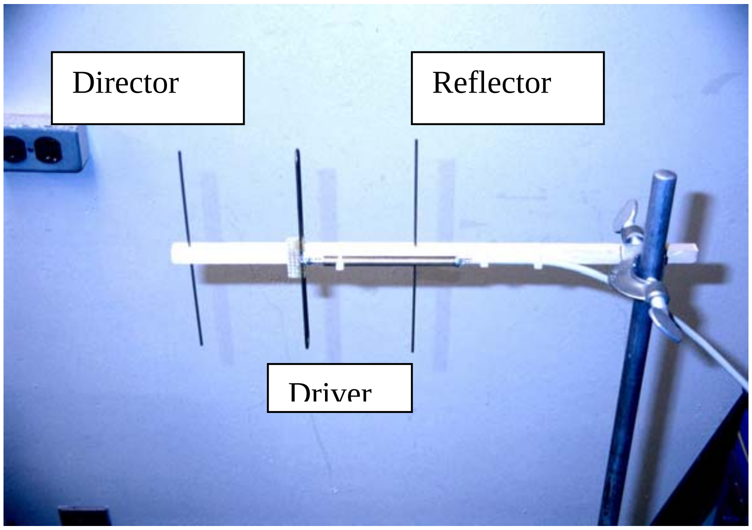

Figure 4. 915 MHz Yagi antenna.

A three-element 6 DB gain YAGI antenna was developed and used for the experiment. See Appendix A for specifications.

The YAGI antenna is a typical example of an Array Antenna. Array Antennas, or simply Arrays, are the configurations of several antennas grouped together to create a directed radiation pattern for required performance.

As shown in Figure 5, there are three key components on a YAGI antenna. These are the reflector, the driver and the director. This arrangement produces a RF beam along the direction of the director.

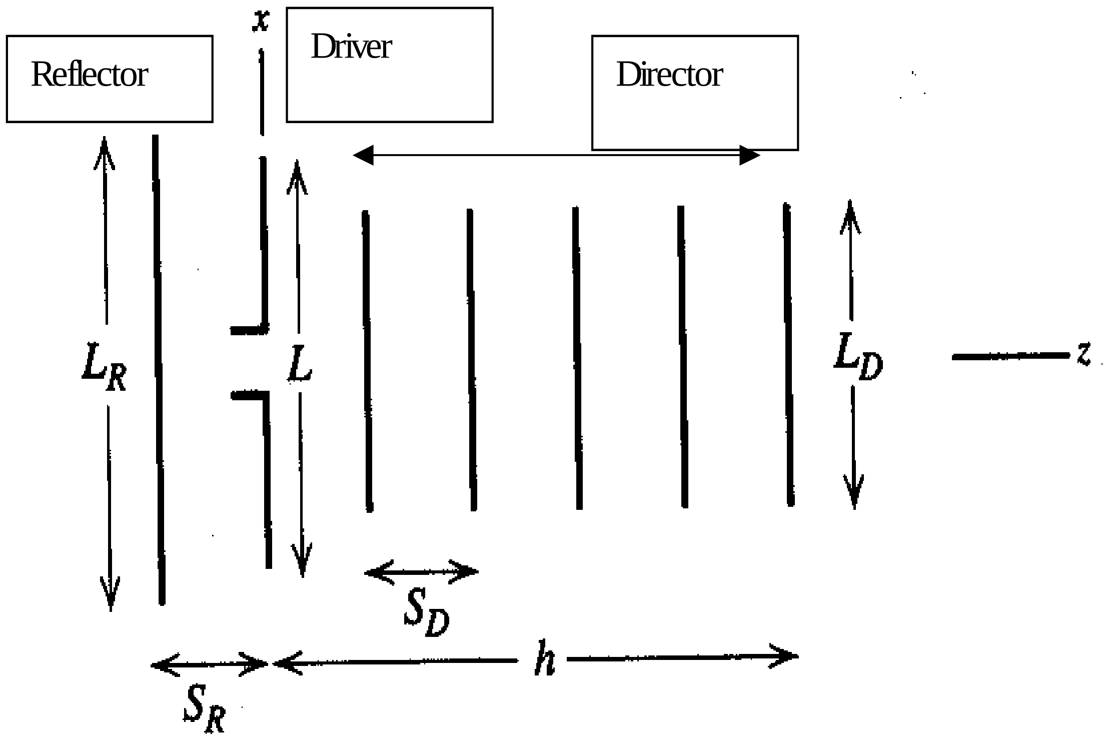

Figure 5. Yagi antenna and components' relative spacing. [from Ref. 6]

L_R: Length of the Reflector
L: Length of the Driver
L_D: Length of the Director
S_R : Spacing of the Reflector
S_D : Spacing Of the Director
h: Director distance

The driver radiates RF power symmetrically to right and left sides of the antennas. The reflector is a parasitic element, which suppress the energy traveling towards left enhancing the energy along the director. The last element of the YAGI antenna is the director. Even though it is a reflector, it is called as director because it comes after the driver, towards the radiation direction, and it has a smaller length than driver.

As mentioned earlier, the gain of our YAGI antenna is 6 dB and the two factors, which contribute to the gain of a YAGI antenna, are the distance between the reflector (S_R) and the driver and the number of directors (N). [Ref.6]. More detailed description can be found in Appendix A.

As shown in the following Figure 6, the addition of directors up to 5 or 6 elements gets more effective increasing of gain in dB. But after a diminishing point the rate of increase begins to decrease, because the excitation of Yagi antenna is not unique through elements and the amplitude of the current gets smaller on the far elements. The increase of the gain as a function of number of directors can be shown by the curve in Figure 6.

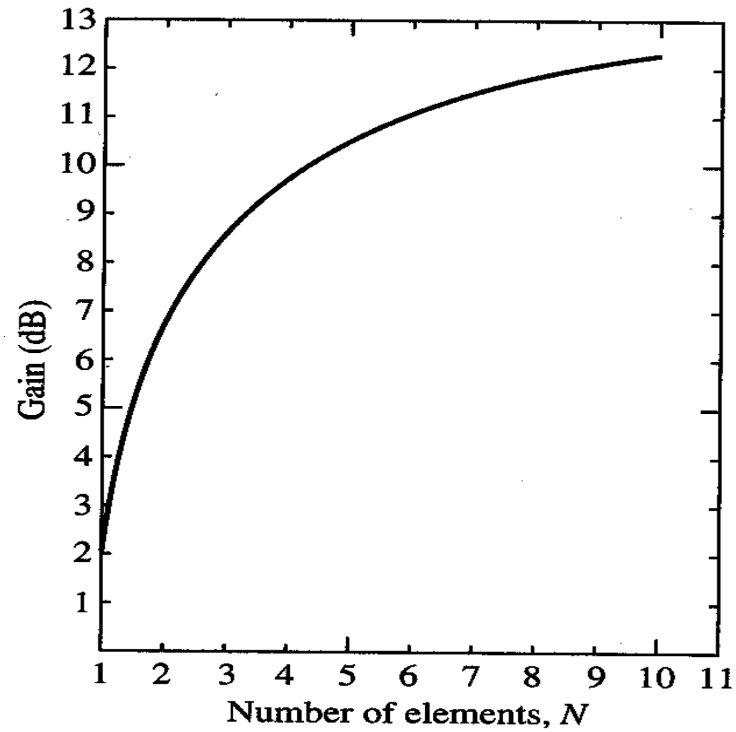

Figure 6. The Relation between gain and #of elements. [fromRef.6]

3. Transceivers

MDS iNET 900 wireless transceivers, Figure 7, were used as the primary image transfer apparatus in the experiment.

Figure 7. MDS iNET 900 Transceivers.

Specifications for these devices can be found in Appendix B. A summary of the iNET 900 capabilities are listed below:

Frequency Bands: 902-928 MHZ ISM Band

Data Rate: 1,200-115,200 bps serial ports

Carrier Power: 20 to 30 Dbm (.1 to 1 Watt)

Interfaces: Ethernet RJ-45, RS232 Serial

Power Requirements: 10-30 Vdc, 13.8 nominal

Management Protocols:

HTTP: embedded web-server

Telnet: remote management

SNMP

MDS Netview

Operating System: Linux

MDS iNET 900 transceivers are designed to operate in a master-station relationship, see Appendix B.

Transceiver attached to the receiver end is capable of measuring the signal strength in dBm.

THIS PAGE INTENTIONALLY LEFT BLANK

II. EXPERIMENTAL SET UP

A. INTRODUCTION

In the initial stage of the experiment, the image transfer was achieved using 2.4 GHz transceivers located close proximity in the laboratory. However, we found that the free space communication signal strength was reduced –95 dB at only 50 ft. This not sufficient for long range image transfer. Thus, we decided to lower the carrier frequency to 915 MHz.

B. SYSTEM ARCHITECTURE

The system, which is configured in this thesis, consists of an IR-160 infrared camera, monitor, RS-232 serial port, wireless transceivers, antennas, 12 volt batteries and a laptop computer as a controlling and storage unit.

The experimental setup used for the IR image transfer is shown in Figure 8. The receiving antenna along with the transceiver and the laptop computer was assembled on a moveable cart for range measurements. The camera and the transmitting antenna / transceiver were located at a fixed position.

Figure 8. Experimental setup used for IR image transfer.

The first step for wireless transfer of images is to connect all the components with the same protocol. The camera and transceiver are connected via RS-232 serial cable since the IR camera only output a serial signal. In the transceiver there is an additional connection available for a, LAN connection for TELNET line to reach the transceiver's management system. The antennas are connected to the transceiver and the receiver by their link line via antennas feeding cable.

The command for capturing and downloading the image is sent to the camera from the computer via RS-232 link and UDP packets. The command is first sent to the transceiver attached to the computer through RS-232 cable as a serial data. This serial data is converted to packet - sized information in the transceiver and passed to the antenna. Trough the free space it sent to the receiver antenna as a UDP packet. The information received by the receiver antenna in UDP packet format is sent to the transceiver connected to the camera. This information is converted to serial data and passed to the camera via RS-232 serial link. To get the captured image to the host computer, the reverse order is followed.

C. COMMUNICATION SPECIFICATIONS ON THE COMPUTER

The WINDOWS operating system is adequate to establish the communication link between the IR –160 camera, host computer through RS-232 serial port and transceivers. After proper hardware connections explained in the previous section, the following steps will explain the procedure for establishing the wireless communication link.

a. From the START menu, choose ALL PROGRAMS, continue with ACCESSORIES, COMMUNICATION and HYPER TERMINAL.

b. In the HYPER TERMINAL choose NEW CONNECTION.

c. The configuration of the NEW CONNECTION includes these specific values: 115,200 BAUD; 8 BITS; NONE PARITY; 1 STOP BIT; NONE FLOW CONTROL for setting the protocol for the IR camera.

d. After these steps there is an empty NEW COMMUNICATION – HYPER TERMINAL screen, ready to type the commands on it.

D. COMMUNICATION SOFTWARE OF THE IR CAMERA

IR-160 camera has its own set of command characters for controlling various functions of the camera. Those commands are single ascii characters and one case insensitive.

Table 2 shows the most commonly used commands for communicating with the camera for downloading images. [Ref. 4]. For example, the command "I" is required to download the image to the host computer. After typing " I " on the screen, the statement of " Downloaded Data – Waiting for the Host " is shown on the monitor attached to the camera.

Character	Command	Definition / Description
A	Acknowledge	This command is intent as a method of testing the serial interface. It does not change the operating mode of the camera.
U	Unfreeze	Start Imager run again (If paused)
Z	Freeze / Snapshot	Pause camera on latest image or snapshot 1 new frame if already frozen.
W	White Hot	Hotter targets in the image are BRIGHTER than colder targets.
B	Black Hot	Hotter targets in the image are DARKER than colder targets.
<	Decrease Brightness	Makes image darker.
>	Increase Brightness	Makes image brighter.
I	Download Image	Transmits a 8 Bit grayscale PGM file via X Modem to the host.

Table 2. Frequently used IR camera commands.

At this point, it is necessary to define the "host address" which is achieved by the following steps.

a. Open “ Transfer Menu “

b. Click on “ Receive File “

c. wreceiving protocol.

d. Click on “ RECEIVE “ button.

e. Give a file name with the “ pgm “ extension to save the downloaded image. (Note that the extension of the file name must be “.pgm”)

After these steps transferring process starts and the progress can be monitored on the monitor attached to the camera. The transfer of an image takes approximately about 3 seconds.

In order to view the downloaded image, a software program (IRFAN VIEW) suggested by the camera manufacturer is employed. This program can be downloaded from the Internet using the site: www.irfanview.com.

E. TRANSCEIVER COMMUNICATION SPECIFICATIONS

The software provided by the transceiver manufacturer can be used to setup the transmitter and the receiver. This menu driven management system software is used for establishing a communication line between ”Access Point“ and “Remote Unit”. First, the same network name must be given for both “Access Point” and “Remote Unit” in addition to the basic configuration defaults in Reference 9.

Second, the terminal emulator (Hyper Terminal) settings are configured. The followings are Hyper Terminal settings required for establishing the link.

Terminal Emulation:	VT100
Data Speed:	19200 bits per second(bps)
Data Format:	8 bits data, no parity, 1 stop bit
Flow control:	None

Third, point to point and serial to serial application configurations are set by the help of the TELNET protocol. The table below shows the serial port configurations for point-to- point application.

MENU ITEM	TRANSCEIVER	RECEIVER
Status	Enabled	Enabled
Data Baud Rate	115200	115200
Flow Control	None	None
Serial Mode	Seamless	Seamless
SIFD	4	4
IP Protocol	UDP	UDP
Remote IP Address	192.168.1.3	102.168.1.1
Remote IP Port	30011	30011
Local IP Port	30011	30011

Table 3. Serial port configuration [from Ref.9]

In order to monitor received signal strength and signal-to-noise ratio, we employed LAN input of the transceiver using a crossover cable. The images were downloaded using the com1 port of the transceiver.

THIS PAGE INTENTIONALLY LEFT BLANK

III. EXPERIMENTAL RESULTS

A. SELECTION OF RF CARRIER FREQUENCY

It is important to select the proper RF carrier frequency to achieve long range image transfer under various conditions. Our intent was to transfer images when the transmit and receive antennas are blocked by obstacles such as walls and trees to emulate urban and terrain environments. Due to the readily availability of 2.4 GHz RF links, the image transfer system was initially developed using this frequency. However, it was found that at 2.4 GHz the range of transmission was around 50 ft with its line of site and no obstacle between antennas. The connection between camera and the computer was lost after 50 ft range. The reason of this high loss is explained by the “Gibson Building Wall Propagation Loss Model”. [Ref.10], Figure 9.

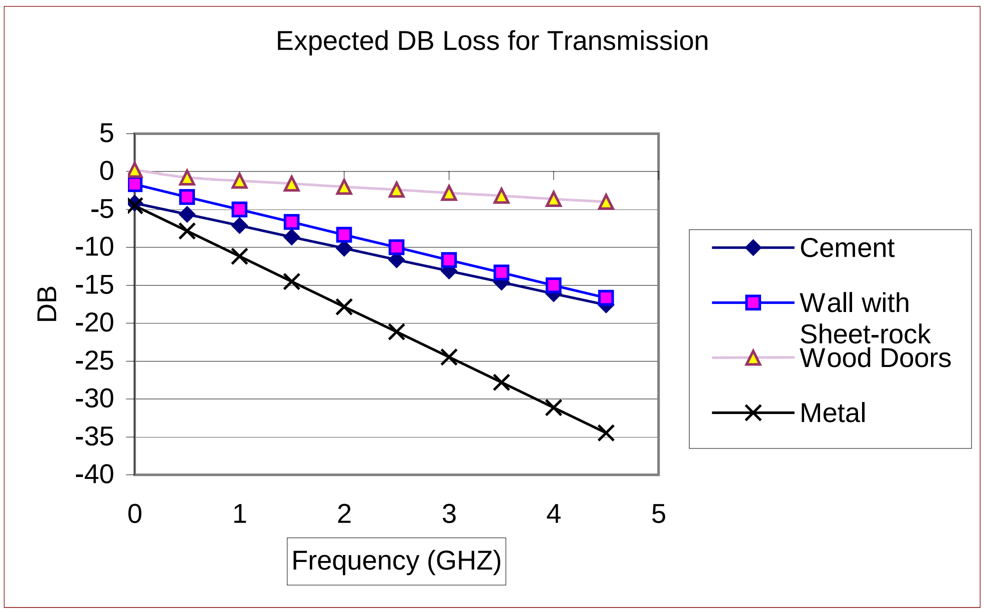

Figure 9. RF Transmission through different materials [from Ref. 10].

The curves in Figure 9 were observed by the computing formula 3.1.

$$E(R_i) = \frac{\tau_1 \tau_2}{4\pi (R_i)} e^{-(\alpha_2 R_2 + j(\beta_0 (R_1 + R_3) + \beta_2 R_2))} \qquad (3.1)$$

Where;

$E(R_i) \equiv$	Electric Field measured at the Equivalent Source Distance
$R_i \equiv$	Equivalent Source Distance
$\tau_1\tau_2 \equiv$	Transmission Coefficients
$\alpha_2 \equiv$	Attenuation constant for lossy dielectric material of the wall
$R_1 \equiv$	Distance from source to the wall boundary
$R_2 \equiv$	Refractive distance through the wall
$R_3 \equiv$	Distance from wall boundary to point of interest
$\beta_0 \equiv$	Phase constant of free space
$\beta_2 \equiv$	Phase constant of the wall

As shown in the graph, the larger the carrier frequency the bigger the loss through all the materials used in the study. For example, the loss through a concrete wall is about –12 dB at 2.4 Ghz which reduces to about –6 dB at 915 MHz, a commonly used ISM frequency. Thus, to overcome the RF losses at 2.4 GHz carrier frequency, we decided to build the system using 915 MHz carrier frequency.

To test the system performance, we conducted several range measurements through the free space and through various obstructions including cement, wood, trees, etc…

B. INDOOR RANGE MEASUREMENTS

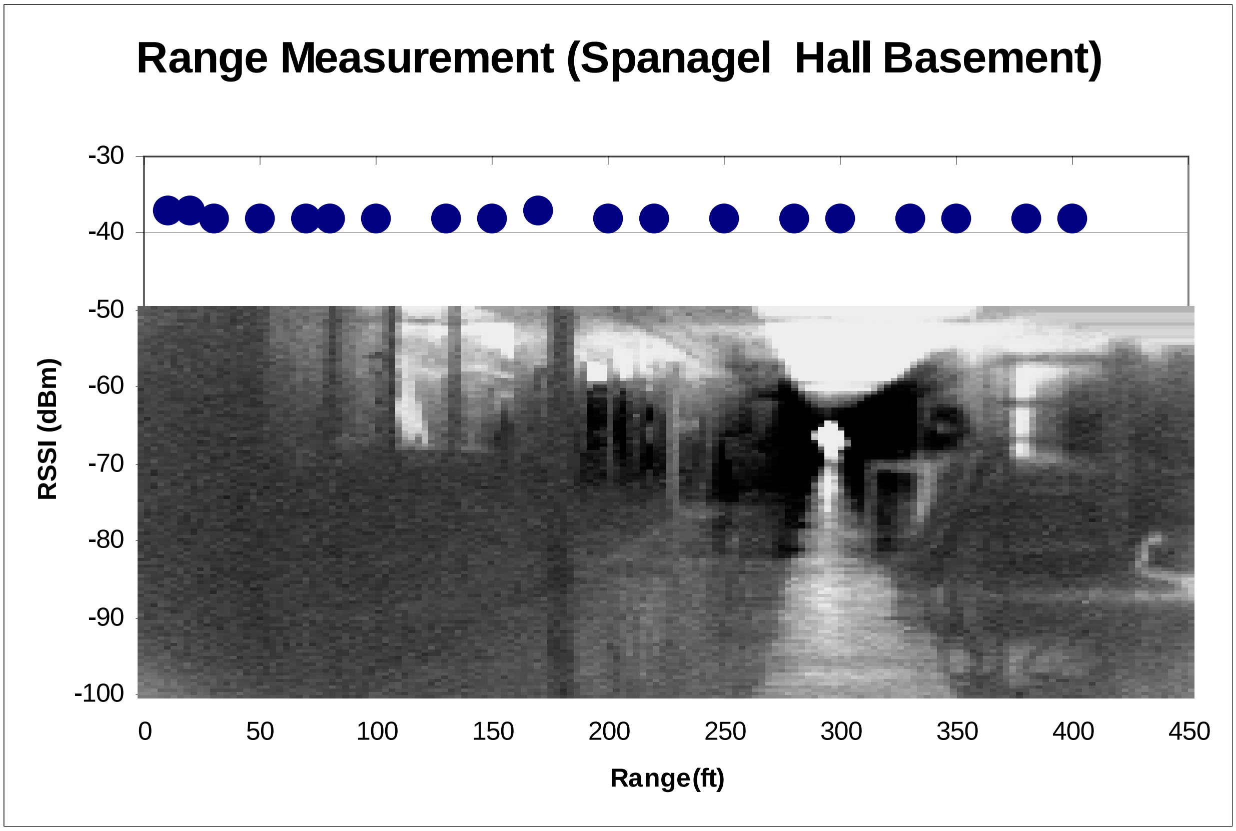

Figure 10. Range Measurements in Spanagel Hall basement

Our initial indoor baseline measurement was conducted at the Naval Postgraduate School, in the basement of Spanagel Hall. This provided both free space (up to 400 ft) and plenty of walls to obstruct the antenna (see Figure 10). The camera and the computer were positioned at the ends of the corridor with the antennas facing to each other. 19 KB images were transmitted successfully in about 3 secondup to the maximum free space range available (400 ft). The measured received signal strength (RSSI) was observed to be around –40 dBm.

The RSSI values span between –38 dBm and –40 dBm. There is not much loss through the hallway and the IR images can be transferred from any point along the distance.

The darker circles of Figure 11 show the measured signal strength as a function of distance when the two antennas are facing each other and the elements are on the same plane, horizontally polarized.

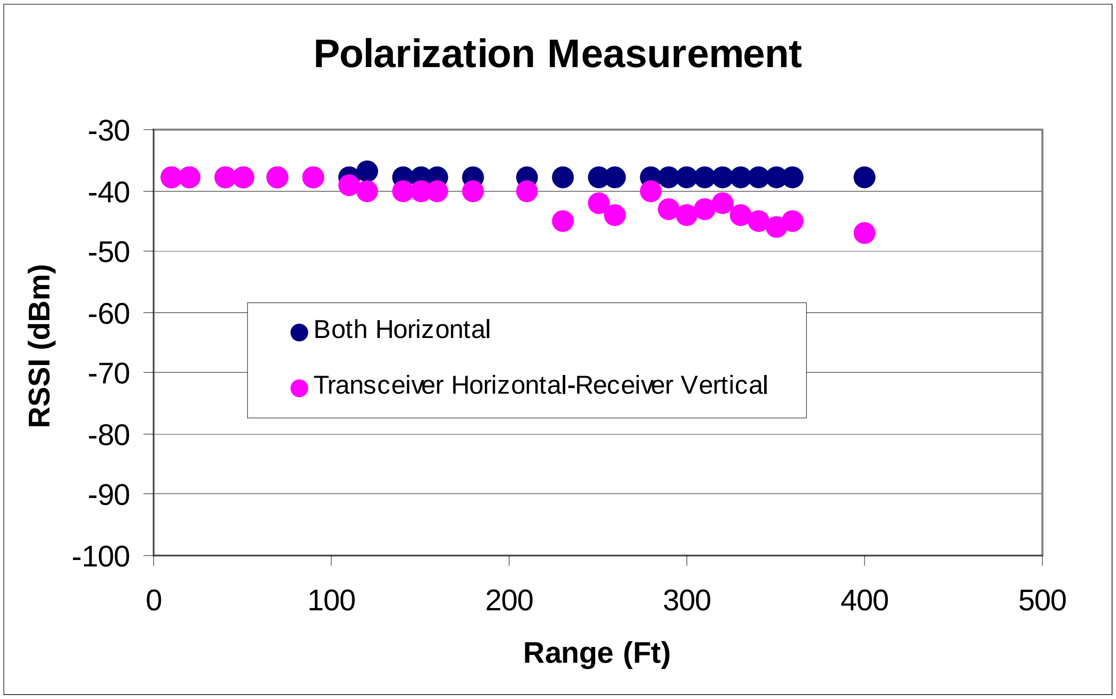

Figure 11. Free Space Range Measurements under different polarizations of the two antennas

To determine the effects of antenna polarization on the signal strength we measured the received signal strength when the planes of the antennas were perpendicular to each other. The results are shown by the light circles in Figure 11. It can be seen that, there is a slight attenuation of the signal as the distance increases. The results indicate that up to 400 ft free space image transfer is not affected by the polarization of the two antennas. Note that the transceivers can successfully communicate up to –95 dBm which is well below the observed signal strength at 400 ft.

C. RANGE MEASUREMENTS THROUGH MULTIPLE OBSTRUCTIONS

As discussed in [10], the loss through multiple walls varies with the number of walls. The threshold value of our system is around –95 dBm. For range measurements with obstructions, the camera was located in the lab (the left most star in the inset of Figure 12) and the receiver was moved along the corridor. Figure 12 shows the signal

strength as a function of distance along the corridor. (The zero distance corresponds to when the two antennas were located at the same place on either side of the wall.) The loss from –30 dBm to –60 dBm is due to the relatively thick wall, which separates the lab from the corridor. As the receiver moved away from the camera along the corridor, the signal strength jumped to lower and lower values as more and more walls obstructs the signal as schematically illustrated in the inset.

The signal strength reduced to –95 dBm at 350 ft where the image transfer failed.

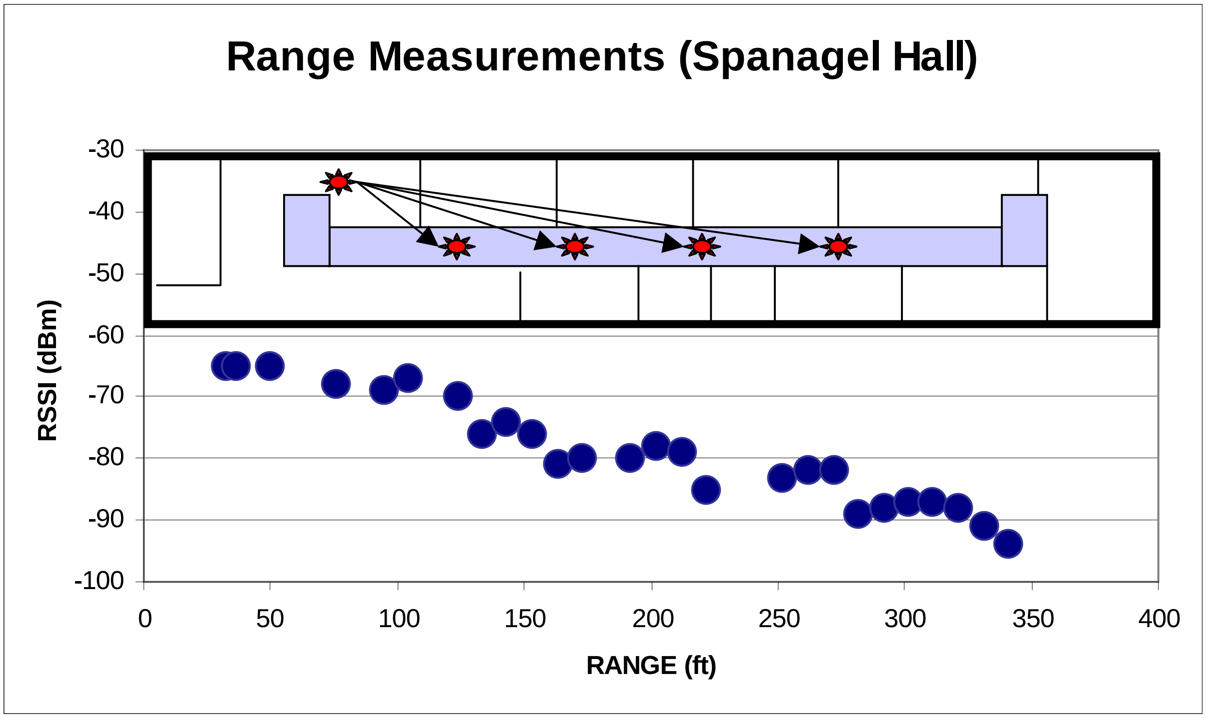

Figure 12. Range Measurements in Spanagel Hall

D. RANGE MEASUREMENT IN OPEN FIELD

In this experiment the area between Spanagel Hall and the Library was chosen to simulate an urban area. The inset in Figure 13 shows a picture transmitted over 1000 ft in free space. The camera and receiver were set in front of Spanagel Hall; and the library, respectively. The image transfer was achieved in about 3 seconds similar to the previous experiments.

The signal strength as a function of distance is shown in Figure 13. It can be seen that the signal strength remains nearly the same for over 1000 ft indicating the effectiveness of 915 MHz for long range image transfer This measurement indicates that in open space we should be able to transfer distances over several miles.

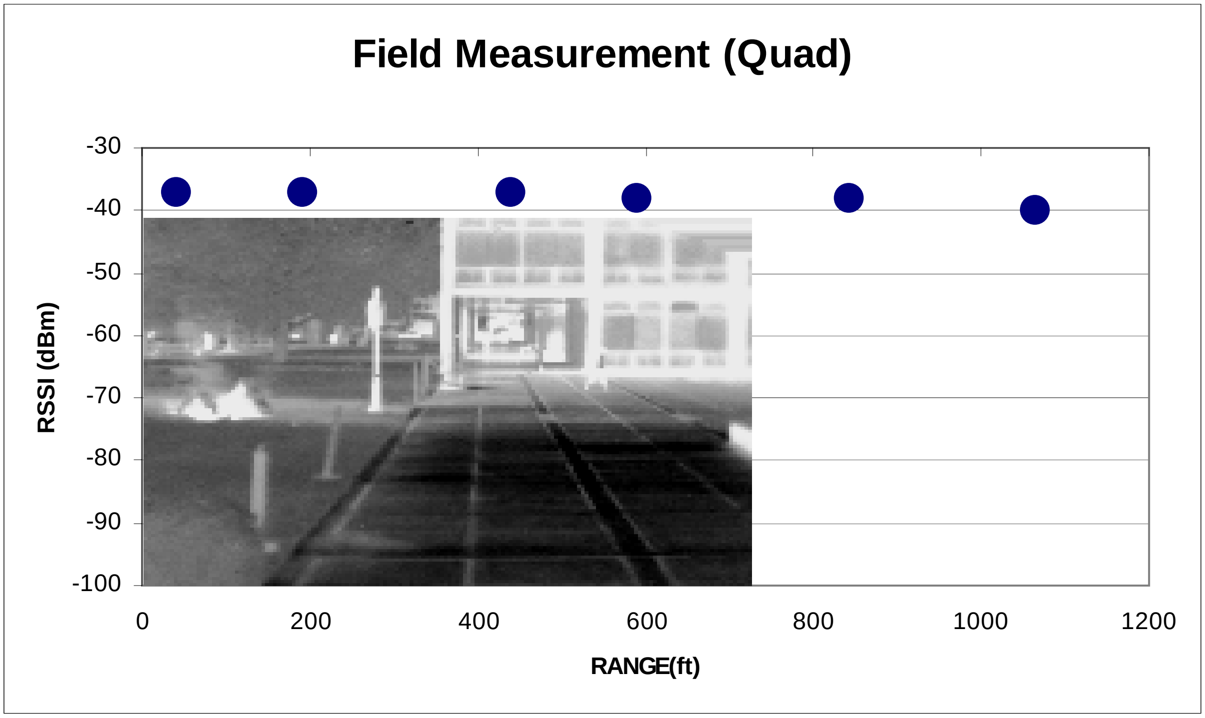

Figure 13. Outside Field Measurements

IV. CONCLUSIONS AND FUTURE WORK

A. CONCLUSIONS

There are three primary conclusions that can be made based on this thesis work.

- The first is about the frequency issue for wireless image transfer. The experimental results show that 915 MHz is best suited for free space transmission as well as through obstacles. Data shows that the signal loss occurs for free space transfer is about –5 dBm for 1000 ft. This implies that the system is capable of image transfer over several miles in free space. In addition, we have observed that the system is capable of transferring images when the antennas are obstructed by several walls.
- The second is that a YAGI antenna under different polarizations the shows a loss is around 8 dBm. This result shows that this system is suitable for used on autonomous vehicles under varying antenna orientations.
- The third is the use of MDS transceivers allows the received images to be accessed over the internet.

B. FUTURE WORK

Future work should include:

- A detailed assessment of the system capability for transferring images under urban environments.
- Determine maximum free space image transfer range
- Measure antenna polarization effects through obstructions
- Investigate any security issue associated with RF communication links

THIS PAGE INTENTIONALLY LEFT BLANK

APPENDIX A. ANTENNA SPECS

Scaled NBS 3 Element YAGI #2		
Freq.	0.915	GHz
Wavelength	327.87	mm
Baseline Freq	0.903	GHz
Baseline WL	332.23	mm

	Baseline (mm)	Length (wave)	Length (mm)	Half Len (mm)	Pos (wave)	Pos (mm)
REFLECTOR	159	0.479	156.91	78.46	0	0
Separation	66.45	0.2	65.58			
DRIVEN ELEMENT	145.4	0.438	143.49	71.75	0.2	65.58
Separation	66.45	0.2	65.58			
DIRECTOR1	143.4	0.432	141.52	70.76	0.4	131.16

Folded dipole DE	mm	inch
Fold Sep	12	0.472
Full Arc Circle	37.7	1.484
MidArc - MidArc	150.34	5.919
Drive Pt. Gap	3	0.118
Tot Rod Len	297.69	11.72
Rod End to MidArc	73.67	2.9

THIS PAGE INTENTIONALLY LEFT BLANK

APPENDIX B. INET 900 MDS SPECS AND TYPICAL APPLICATION

General	
Configurations:	**Access Point/Remote Dual Gateway**
	Serial and Ethernet
	Remote Serial Gateway
	Serial only
	Remote Ethernet Bridge
	Ethernet only (with multipdrop capability)
Frequency Bands:	902-928 MHz ISM band
Data Rate:	512/256 Kbps user configurable air link
	1,200-115,200 bps serial ports
Spreading Mode:	Frequency Hopping Spread Spectrum
Coverage Range:	Up to 30 mi. (40 Km.)
Transmitter	
Carrier Power:	0.1 to 1 watt (20 to 30 dBm)
Output Impedance:	50 Ohms
Modulation:	CPFSK (Continuous Phase FSK)
Occupied Bandwidth:	316.5 kHz
Receiver	
Sensitivity:	-92 dBm @ 512 Kbps with 10^{-6} BER
	-99 dBm @ 256 Kbps with 10^{-6} BER
Interfaces	
Ethernet Port:	10BaseT, RJ-45
LEDs:	Lan, Com1, Com2, Power, Link
Serial Ports:	RS-232/V.24, DB-9F, DCE
	RS-232/V.24, DB-9M, DTE
Antenna:	TNC connector (female)

Environmental	
External power supply:	48 Vdc, 110/220 Vac
Humidity:	95% at 40°C (104°F) non-condensing
Temperature Range:	-30°C to +60°C (-22°F to +140°F)
Current Consumption:	Rx: 2.8W from 10.5 to 24 Vdc
	Rx: 3.5W from 24.5 to 30 Vdc
	Tx: 8W from 10.5 to 24 Vdc
	Tx: 9W from 24.5 to 30 Vdc
Input Power:	10.5-30 Vdc (13.8 Vdc nominal)
Physical	
Mounting Options:	Flat surface mount brackets, DIN rail, 19" rack (1U high)
Case:	Die Cast Aluminum
Dimensions:	3.15 H x 17.2 W x 11.2 D cm
	(1.25 H x 6.75 W x 4.5 D in.)
Weight:	908 g (2 lb.)
Network Management	
HTTP (embedded web server), TELNET, local console, SNMPv1/v2/v3, MIB II, Enterprise MIB	
SYSLOG	
MDS NETView MS™	
Agency Approvals	
FCC Part 15.247	
UL/CSA Class 1 Div. 2 approved* (UL 508, UL 1604)	
IC	
Protocols	
Wireless:	CSMA/CA Wireless Protocol with Collision Avoidance
Ethernet:	IEEE 802.3
	Spanning Tree (Bridging)
	IP (DHCP, ICMP, UDP, TCP, ARP)
Serial:	PPP
	Encapsulation over IP for serial async multidrop protocols including Modbus, DNP.3, DF1, BSAP.

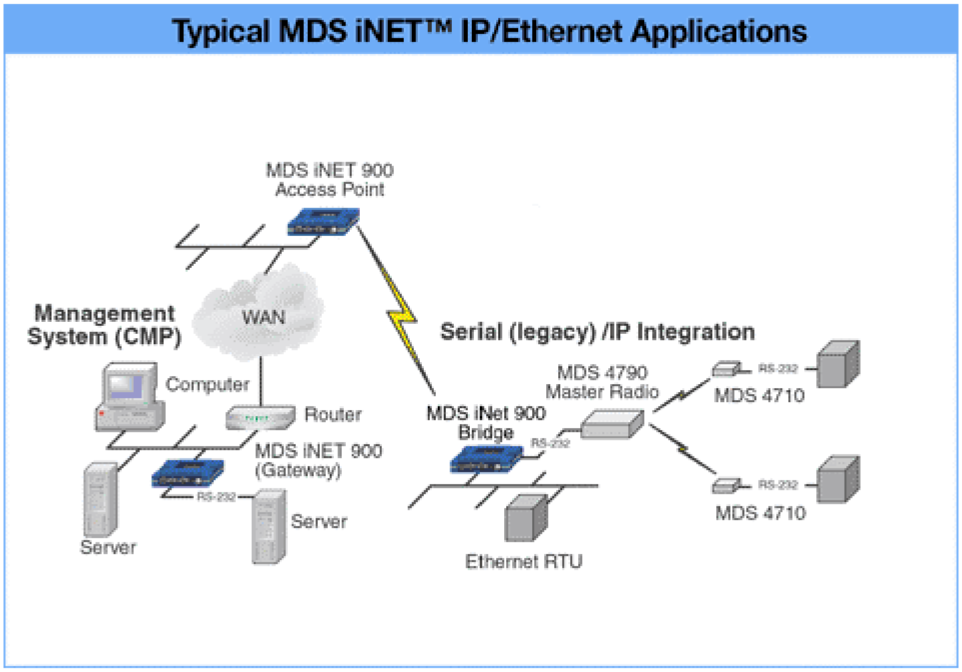
Typical MDS iNET™ IP/Ethernet Applications
MDS iNET 900
Access Point
Management
System (CMP)
WAN
Computer
Router
MDS iNET 900
(Gateway)
RS-232
Server
Server
Serial (legacy) /IP Integration
MDS 4790
Master Radio
MDS iNet 900
Bridge
RS-232
MDS 4710
RS-232
MDS 4710
RS-232
Ethernet RTU

THIS PAGE INTENTIONALLY LEFT BLANK

LIST OF REFERENCES

1. Jha, "A. R. Infrared Technology", John Wiley & Sons Inc., 2000.

2. Schlessinger, Monroe. "Infrared Technology Fundamentals", 2nd Edition, Marcel Dekker Inc., 1995.

3. Kaplan, Herbert. "Practical Applications of Infrared Thermal Sensing and Imaging Equipment", 2nd Edition, SPIE Optical Engineering Press, 1999.

4. Infrared Solutions Inc., IR - 160 Thermal Imager [http://www.infraredsolutions.com], October 2003.

5. Computer Tips, RS – 232 Serial Port, [http://www.ctips.com/rs232.html], October 2003.

6. Stutzman, Warren L. and Thiele, Gary A., "Antenna Theory and Design", 2nd Edition, John Wiley & Sons Inc., 1998.

7. Walters, Don. PH – 4274 Course Notes. September 2003.

8. Microwave Data Systems Inc., "MDS iNET 900 User's Guide", August 2003.

9. Thad B. Gibson and David C. Jenn. "Prediction and Measurement of Wall Insertion", *IEEE NPS 1995*

10. X. Gu, G. Karunasiri, G. Chen, U. Sridhar, and B. Xu. "Determination of thermal parameters of microbolometer using a single electrical measurement". Applied Physics Letters, 02.13.1998.

THIS PAGE INTENTIONALLY LEFT BLANK

INITIAL DISTRIBUTION LIST

1. Defense Technical Information Center
   Ft. Belvoir, Virginia

2. Dudley Knox Library
   Naval Postgraduate School
   Monterey, California

3. Chairman (Code PH)
   Department of Physics
   Naval Post Graduate School
   Monterey, California

4. Gamani Karunasiri
   Naval Post Graduate School
   Monterey, California

5. Richard M.Harkins
   Naval Post Graduate School
   Monterey, California

6. Deniz Harp Okulu Komutanligi
   Tuzla / Istanbul, TURKEY

7. Ali Ata
   Inonu Mah.Lise Cad.No7
   Odemis, Izmir, Turkey